

# Broadband resonant calibration-free complex permittivity retrieval of liquid solutions

Dmitry S. Filonov<sup>1,2,=</sup>, Egor I. Kreto<sup>1,=</sup>, Sergei A. Kurdjumov<sup>1</sup>, Viacheslav A. Ivanov<sup>1</sup> and Pavel Ginzburg<sup>2</sup>

1. Department of Nanophotonics and Metamaterials, ITMO University, St-Petersburg, Russia, 197101

2. School of Electrical Engineering, Tel-Aviv University, Tel-Aviv, Israel, 69978

=contributed equally

Material susceptibilities govern interactions between electromagnetic waves and matter and are of a crucial importance for basic understanding of natural phenomena and for tailoring practical applications. Here we present a new calibration-free method for relative complex permittivity retrieval, which allows using accessible and cheap apparatus and simplifies the measurement process. The method combines advantages of resonant and non-resonant techniques, allowing to extract parameters of liquids and solids in a broad frequency range, where material's loss tangent is less than 0.5. The essence of the method is based on exciting magnetic dipole resonance in a spherical sample with variable dimensions. Size-dependent resonant frequencies and quality factors of magnetic dipolar modes are mapped on real and imaginary parts of permittivity by employing Mie theory. Samples are comprised of liquid solutions, enclosed in stretchable covers, which allows changing the dimensions continuously. This approach allows tuning magnetic dipolar resonance over a wide frequency range, effectively making resonance retrieval method broadband. The technique can be extended to powder and solid materials, depending on their physical parameters, such as granularity and processability.

## I. INTRODUCTION

Retrieval of material parameters is of a crucial importance for a broad range of applications, based on propagation of electromagnetic waves and their interactions with matter<sup>1</sup>. Material susceptibilities govern constitutive relations, substituting Maxwell's equations and enabling to find their unique solutions. While a general concept of the parametric retrieval is quite universal and is always based on probing a structure's response to an applied electromagnetic field, practical constraints set numerous technical limitations and give rise to development of many complementary experimental techniques.

The set of experimental methods for parametric retrieval is rather large, but their vast majority can be divided into two main groups: resonant<sup>2</sup> and non-resonant techniques<sup>3</sup>. Each group has its own advantages and drawbacks: while non-resonant methods are naturally broadband, resonant approaches are restricted to a limited frequency range with an advantage to provide more accurate data. Hereinafter main approaches will be briefly surveyed, and main limitations will be underlined. Regardless of the type of methods, most of them require using of a vector network analyzer (VNA) to perform measurements of the reflection parameters at a certain frequency range and specialized equipment for samples' positioning or shaping is also needed. These requirements are related to some technical constraints in methods' implementation.

### Non-resonant methods

#### Open-ended coaxial probe

A widespread commercially available open-ended coaxial probe technique<sup>4</sup> is commonly employed for quality control<sup>5</sup>, antenna design<sup>6</sup> and in biomedical applications<sup>7</sup>. Specially designed probes are immersed in a liquid or placed on top of a solid and  $S_{11}$  parameter (complex-valued reflection) is measured. Accuracy of the method is constrained by a three-step calibration process. Interpretation of the results requires non-trivial processing, usually performed with quite a sophisticated software.

### Rectangular waveguide

Another widely used method for parametric retrieval utilizes a waveguide configuration. Here a sample is inserted into a two-port waveguide section, connected to a VNA. The retrieval is based on relating S-parameters to the impedance of an unknown material<sup>8,9</sup>. This approach allows extracting both permittivity and permeability of a dielectric slab by employing relatively straightforward mathematical formulation<sup>10,11</sup>. Commonly used Nicolson-Ross-Weir method is well justified for solid samples, which are thicker than half of a wavelength. However, waveguide geometry has significant limitations in application to liquid solutions, nevertheless cuvettes can be designed to host liquids. Solid samples also require special shaping in order to fit waveguide cross-sections. Furthermore, constraint of single mode operation of a waveguide limits the acquisition bandwidth, provided by a single device. Usage of several waveguides (one per each frequency band) is possible, but ends up by relatively high investments in relevant equipment.

### Transmission lines

Another widely used approach utilizes transmission line geometry. A dielectric sample is placed on top of a microstrip line, connected to VNA ports. S-parameters are then related to complex permittivity of a sample<sup>12</sup>. This approach allows performing extraction in a wide frequency range (~0.05-75 GHz) and is also applicable to lossy materials. Accurate retrieval requires a VNA, which might be quite an expensive, if high frequency measurements are targeted. Investigation of liquid solutions also demands usage of cuvettes.

### Resonant Methods

#### Resonant cavity

Cavity configuration is one of the most commonly used resonant methods. It allows to extract permittivity values from resonant responses of a cavity, measured with and without a sample, incorporated inside it<sup>13,14</sup>. Here, the permittivity can be extracted only at a single (resonant) frequency. It is worth mentioning, however,

several extensions, where adjustable resonant cavities are reported<sup>15,16</sup>.

### Combination of resonant and non-resonant methods – Our Proposal

The beforehand presented survey demonstrates strengths and limitations of several existent methods. The proposed experimental technique takes advantages of resonant and non-resonant approaches simultaneously. The essence of the method is Mie theory, which allows to obtain analytical solutions to a problem of electromagnetic scattering on a dielectric sphere<sup>17</sup>. Mie solutions link between geometry, material parameters of a sphere and resonant peaks in its scattering spectrum. In particular, resonant condition for the first magnetic (dipolar) mode is given by:

$$\lambda_{res} \approx \sqrt{\epsilon} \cdot D \quad (1)$$

Eq. 1 assumes relative permeability of the sphere  $\mu=1$ <sup>18</sup>. If a broad scattering spectrum is observed, the first resonance at the lowest frequency obeys the condition of Eq. 1. It is worth noting that Eq. 1 allows identifying a real part of the permittivity, while its imaginary component can be found by analyzing the spectral widths. Both radiation and material loss contribute to this value. In addition, overlapping resonances can furthermore complicate the direct retrieval. A complimentary method can be based on Kramers-Kronig relations linking real and imaginary parts via an integral relation. However this approach has significant limitations when available experimental data has a finite bandwidth and a relatively small number of experimental points forms the spectra<sup>19</sup>. Here we found the first method of spectral resonance width to be more accurate, if several simplifying assumptions are made: (i) material losses prevail over radiation leakage, (ii) spectrum has well defined and separated resonant features. In this case, the imaginary part of permittivity can be calculated via Q-factor relation:

$$\epsilon'' = \frac{\epsilon'}{Q} \quad (2)$$

Based on the formulation of Eqs. 1 and 2, we propose a new technique for parametric retrieval. Our method is calibration-free and does not require expensive additional equipment (apart from a scalar network analyzer, phase information is not mandatory). Furthermore, the data post-processing is transparent and straightforward, which makes the method to be cheap and easy for handling.

## II. METHODS

### Liquid Solutions

In order to retrieve permittivity within a desired frequency range, the diameter of the sphere  $D$  should be varied continuously. This was implemented by using a stretchable latex balloon, enclosing a liquid solution under the test. The volume of the incompressible liquid was controlled with a calibrated injecting syringe, connected to the latex enclosure via a capillary. Schematic representation of the setup is depicted on Fig. 1, while its photograph appears in Fig. 2(a). An empirical relation between the surface tension of the balloon, the pressure, supplied by the syringe, and the overall volume of the sphere was obtained. This apparatus allows achieving almost continuous control over the dimensions, which is the key factor for ensuring broadband operation of this resonance-based method. An additional important technical detail is the shape monitoring of the balloon,

which should be kept as spherical as possible in order to employ Eq. 1 for the permittivity retrieval.

The resonance measurement was made by approaching the structure with a magnetic loop antenna (Fig. 1) positioned on top of the sphere. The antenna's feed was connected to Agilent E8362C VNA and  $S_{11}$  parameter was retrieved. According to Mie theory, the first dip (the lowest in frequency) in the reflection coefficient corresponds to the magnetic dipole mode, which resonance condition is described by Eq. 1. In order to avoid resonance hybridization, the internal resonance of the loop antenna should be engineered to fall outside of the frequency window, where permittivity is aimed for the retrieval. In our case, the loop resonance frequency was about 10 GHz, while all measured resonances of spheres fall within 0.5-4 GHz range.

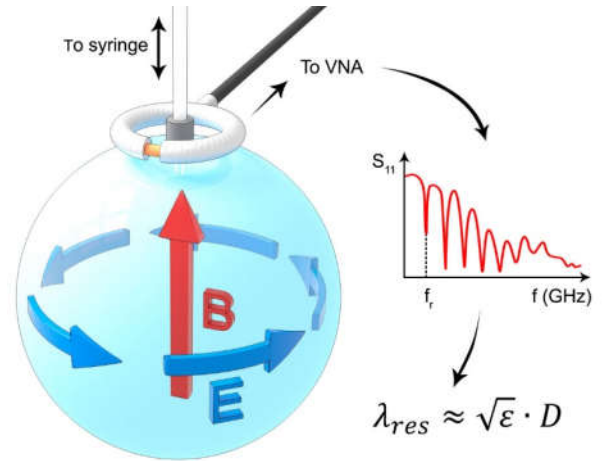


Figure 1. Schematic representation of the experimental setup for extraction of complex permittivity. Arrows illustrate the electric (blue) and magnetic (red) vector fields, corresponding to the magnetic dipole resonance. Sphere's dimensions can be dynamically tuned, shifting the corresponding magnetic dipole resonance in frequency. Non-resonant probe (loop antenna) is connected to a vector network analyser (VNA) and placed above the sphere. Permittivity is retrieved by monitoring spectral dips in the reflection coefficient from the probe ( $S_{11}$ -parameter) –  $S_{11}$  spectrum is schematically depicted in the right inset. Resonant frequency  $f_r$ , corresponding to the dipole magnetic resonance, along with the resonance quality factor, allow retrieval of complex permittivity in a broad spectral range, defined by the set of available sphere's radii.

Numerical simulation was performed first to estimate the accuracy of the proposed method. A spherical thin shell, filled with distilled water, was analyzed numerically with Frequency Domain method, implemented in CST Microwave Studio. Permittivity, obtained with commercial dielectric assessment kit (DAK)<sup>18</sup>, was used as an input to the modeling. Resonant spectra for different sphere's radii were obtained and post-process with the help of Eqs. 1 and 2. In the ideal case, the results of this resonant type of retrieval should provide back the input data, while deviations will indicate systematic errors and inaccuracies. Fig. 2(b) summarizes this investigation - complex permittivity of distilled water in the range of 0.7-5 GHz was retrieved. Liquid's temperature during the measurements was 16.3 degrees Celsius. Three-step calibration was performed, and permittivity was automatically obtained by using commercial software. DAK data is then can be assessed versus the resonant retrieval. It can be seen that the relative systematic inaccuracy of the method is in the range of 5% and provides a

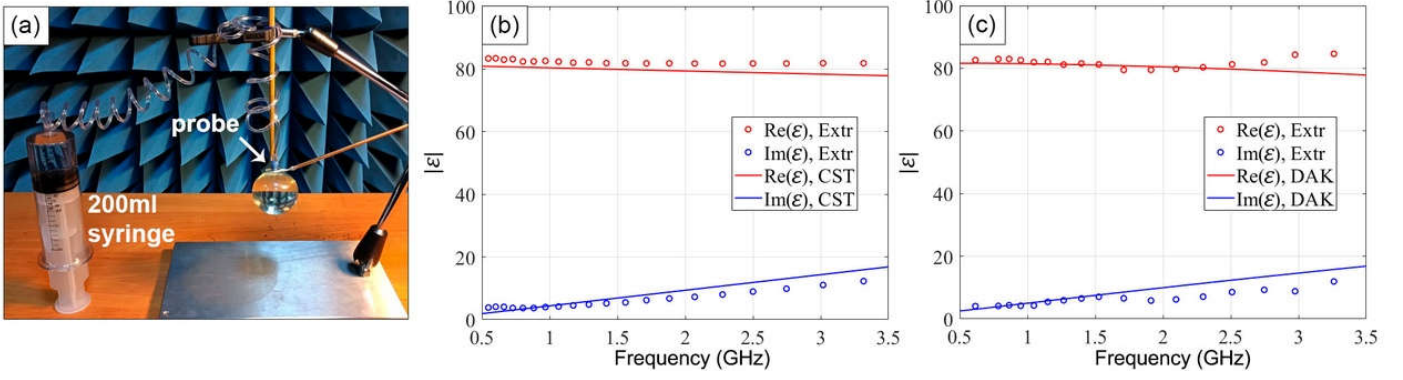


Figure 2. (a) Photograph of the experimental setup for parametric retrieval of liquid solutions. (b) Permittivity spectrum of distilled water - real (red) and imaginary (blue) parts of permittivity. Solid lines – permittivity, extracted with a commercial dielectric assessment kit (DAK). Circles – permittivity, retrieved from numerical modeling with the subsequent post-processing via Eqs 1 and 2. Etalon permittivity (solid lines, DAK extraction) is used as an input to the modeling. Deviations between solid lines and circles demonstrate the accuracy of the method. (c) Complex permittivity of distilled water (red and blue colors stay for real and imaginary parts, correspondingly). Solid lines – values, extracted with DAK. Circles – values, extracted experimentally with setup from panel (a) by fitting resonance conditions, defined by Eqs. 1 and 2.

reasonable approximation of the reality. Deviations grow with the frequency as the result of losses increase. The beforehand mentioned comparison relies on experimental data (DAK method) and not on a tabulated one, in order to perform fair comparison, factoring out a probable influence of the liquid preparation protocol.

After estimating the accuracy of the method numerically, experimental retrieval was performed. Experimental setup is shown in Fig.2 (a). The sphere formed by a shell, made of widely available medical latex, was fastened with threads at the end of a capillary. Its other end was connected to a 200 ml syringe filled with a liquid (distilled water in our case). Sphere's diameter was varied by controlling the volume of the liquid, supplied from the syringe. The loop antenna was placed around the supplying capillary. This place was found to be optimal in terms of ensuring a constant distance between the antenna and the surface of the sphere during changing its dimensions.  $S_{11}$  parameter of the loop antenna was measured with Agilent E8362C VNA. 17 different diameters between 10 and 60 mm were assessed. The obtained data were processed using the same procedure as in the case of numerical modeling (Eqs. 1 and 2). Extracted values of real and imaginary values of permittivity are shown in Fig.2 (c) (red and blue circles) together with reference DAK measurement (solid red and blue lines). Reasonable agreement can be observed, while the deviations become more significant with the frequency increase. The main reason here is losses, which become more significant at higher frequencies.

#### Solid materials

The proposed method can be also applied on solid materials. Here, however, a set of samples with different dimensions should be prepared with available fabrication techniques (e.g. machine milling). Another possible application of the resonance method can be a quality check of materials, where responses of new fabricated samples are compared with an etalon. Here we demonstrate this capability by investigating six identical high-quality ceramic spheres of 15 mm diameter (Fig. 3(a)). The deviation of radii was estimated to be on the order of 1 mm and less, according to calipers. Deviations in resonant locations were observed to be in the range of less than 3% (Fig. 3(b) -  $S_{11}$  spectra, acquired with the same loop antenna probe). Etalon characteristic of the ceramics is 16 for real and 0.642 for imaginary part at 5 GHz frequency).

Calculated values of real and imaginary parts of spheres' permittivities are presented in the Table 1. In all of the investigated

samples the losses are significantly higher than declared, while the real part of permittivity is quite accurate. The hypothesis on the loss mechanism is internal granularity of structures, obtained during the sintering during the fabrication.

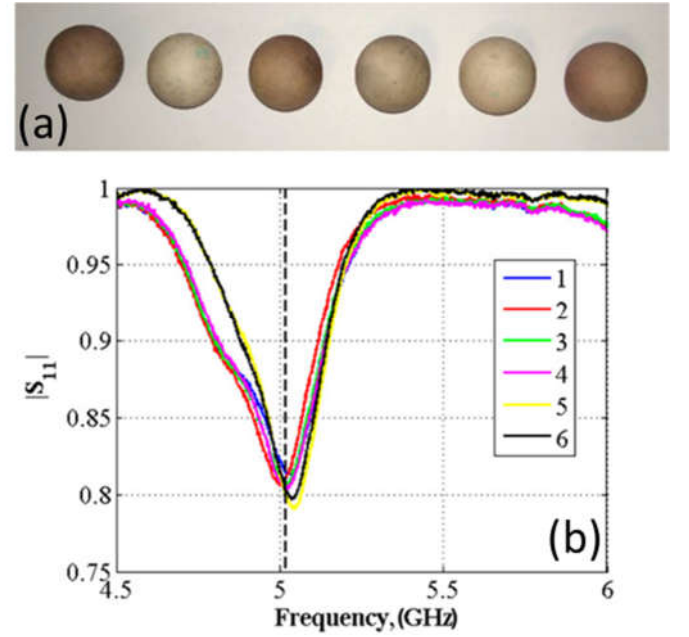


Figure 3. (a) A photo of the ceramic samples. (b) Experimental  $S_{11}$  spectra of the samples. Dashed line shows the average position of the magnetic dipole resonance frequency.

| $N_0$ | $\epsilon'$ | $\epsilon''$ | $\epsilon'$<br>(ref) | $\epsilon''$<br>(ref) | $\Delta\epsilon'$ ,<br>% | $\Delta\epsilon''$ ,<br>% |
|-------|-------------|--------------|----------------------|-----------------------|--------------------------|---------------------------|
| 1     | 15.78       | 0.78         | 16                   | 0.64                  | 1.37                     | 20.88                     |
| 2     | 16.00       | 0.72         |                      |                       | 0%                       | 12.53                     |
| 3     | 15.91       | 0.73         |                      |                       | 0.56                     | 14.10                     |
| 4     | 15.88       | 0.68         |                      |                       | 0.75                     | 6.32                      |
| 5     | 15.73       | 0.54         |                      |                       | 1.69                     | 15.60                     |
| 6     | 15.76       | 0.56         |                      |                       | 1.50                     | 12.54                     |

Table 1. Retrieved real and imaginary parts of permittivity of 6 identical ceramic samples (from left to right, Fig. 3(a)).

#### IV. DISCUSSION

It is important to estimate fundamental limitations of the proposed method. The key parameter here is material losses, which make resonant response of structures to be less pronounced. In order to support this statement, we performed a set of numerical simulations, where the real permittivity was kept constant (80) and loss tangent was varied from  $10^{-4}$  to  $\sim 1$ . The frequency range was taken to be between 0.5 and 3.5 GHz, radius of the sphere is 10mm. Fig. 4 demonstrates the data, there  $|S_{11}|$  values are presented with colors, while vertical and horizontal axes stay for frequency and loss tangent, correspondingly. Three first resonances can be clearly seen up to a point, where losses smear out the resonant behavior. This information is virtually lost for loss tangent starting from about 0.5 and higher. It can be also seen that resonance broadening affects the data already starting from  $10^{-1}$ - $10^{-2}$ , supporting the frequency dependent deviations on Fig. 2 (losses of water grow significantly with frequency).

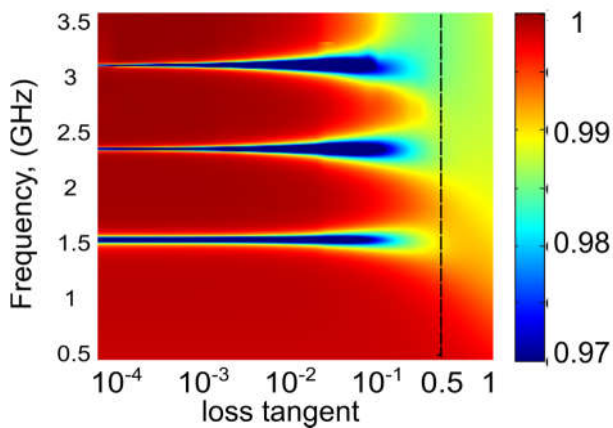


Figure 4. Influence of losses on the resonant retrieval -  $|S_{11}|$  values are presented with colors, while vertical and horizontal axes stay for frequency and loss tangent, correspondingly. Magnetic dipole resonance is the lower branch ( $\sim 1.5$ GHz). The black dashed line shows the range of applicability (0.5 is set as the higher bound for acceptable losses). Real part of the permittivity is 80, radius of the sphere 10mm.

#### V. CONCLUSIONS

We have demonstrated a new calibration-free method for extracting complex material permittivities of liquid solutions. Our methodology combines advantages of accurate resonant and broadband non-resonant approaches. Our design is based on a stretchable enclosure, which allows continuous tuning of sample's (resonant cavity) dimensions. Mie theory is employed to link between resonant conditions, dimensions and material parameters – this is the key for the extraction procedure. The proposed methodology was assessed versus commercially available calibrated tools and showed a good agreement within 5% accuracy over a broad frequency range (0.5-3.5GHz). The main fundamental limitation of the method is related to loss tangent, which cannot access the value of 0.5. Practical difficulties of the implementation are related to mechanical stabilization of samples and accurate maintenance of their spherical shape. Thermal control was found to be also an important factor. The accuracy of the methodology can be further improved if the entire Mie resonance spectra are post-processed and complex-valued S-parameters are taken into account.

The main advantage of the method is its straightforward implementation, clear relation between measured data and the physical origin, and cheap experimental apparatus, required for the experiment.

As an outlook, this new broadband resonant approach can be employed for investigation of different types of materials, such as liquids, powders and solids. Continuous shape variation of a cavity configuration allows performing the permittivity retrieval.

#### References:

- <sup>1</sup> S. Costanzo, *MICROWAVE MATERIALS* Edited by Sandra Costanzo (n.d.).
- <sup>2</sup> J. Krupka, in *Meas. Sci. Technol.* (IOP Publishing, 2006), pp. R55–R70.
- <sup>3</sup> S.L.S. Severo, Á.A.A. de Salles, B. Nervis, and B.K. Zanini, *J. Microwaves, Optoelectron. Electromagn. Appl.* **16**, 297 (2017).
- <sup>4</sup> J.P. Grant, R.N. Clarke, G.T. Symm, and N.M. Spyrou, *J. Phys. E.* **22**, 757 (1989).
- <sup>5</sup> K.M. Donnell, A. McClanahan, and R. Zoughi, *IEEE Trans. Instrum. Meas.* **63**, 1877 (2014).
- <sup>6</sup> D. Filonov, S. Kolen, A. Shmidt, Y. Shacham-Diamand, A. Boag, and P. Ginzburg, *Phys. Status Solidi - Rapid Res. Lett.* (2019).
- <sup>7</sup> A. La Gioia, E. Porter, I. Merunka, A. Shahzad, S. Salahuddin, M. Jones, and M. O'Halloran, *Diagnostics* **8**, 40 (2018).
- <sup>8</sup> A.M. Nicolson and G.F. Ross, *IEEE Trans. Instrum. Meas.* **19**, 377 (1970).
- <sup>9</sup> O. Luukkonen, S.I. Maslovski, and S.A. Tretyakov, *IEEE Antennas Wirel. Propag. Lett.* **10**, 1295 (2011).
- <sup>10</sup> W.B. Weir, *Proc. IEEE* **62**, 33 (1974).
- <sup>11</sup> P.A. Belov, A.P. Slobozhanyuk, D.S. Filonov, I. V. Yagupov, P. V. Kapitanova, C.R. Simovski, M. Lapine, and Y.S. Kivshar, *Appl. Phys. Lett.* **103**, (2013).
- <sup>12</sup> L.F. Chen, C.K. Ong, C.P. Neo, V. V. Varadan, and V.K. Varadan, *Microwave Electronics* (2004).
- <sup>13</sup> V. Review, *Changes* **82**, (1951).
- <sup>14</sup> N. Krismer, D. Silbernagl, M. Malfertheiner, and G. Specht, *CEUR Workshop Proc.* **1594**, 74 (2016).
- <sup>15</sup> D. Gershon, J.P. Calame, Y. Carmel, and T.M. Antonsen, *Rev. Sci. Instrum.* **71**, 3207 (2000).
- <sup>16</sup> X. Fang, D. Linton, C. Walker, and B. Collins, *IEEE Trans. Instrum. Meas.* **53**, 1473 (2004).
- <sup>17</sup> F. Ehrenhaft and L. Lorenz, (1908).
- <sup>18</sup> A.I. Kuznetsov, A.E. Miroshnichenko, M.L. Brongersma, Y.S. Kivshar, and B. Luk'yanchuk, *Science* **354**, aag2472 (2016).
- <sup>19</sup> K.R. Waters, J. Mobley, and J.G. Miller, *IEEE Trans. Ultrason. Ferroelectr. Freq. Control* **52**, 822 (2005).